Hindawi
Advances in Meteorology
Volume 2021, Article ID 6680067, 12 pages
https://doi.org/10.1155/2021/6680067

Research Article

Spatiotemporal Variations of Drought in the Arid Region of Northwestern China during 1950–2012

Wenjun Huang[1,2], **Jianjun Yang**[1,2], **Yang Liu**[1,2] **and Entao Yu**[3,4]

[1]*College of Resources and Environmental Science, Xinjiang University, Urumqi 830046, China*
[2]*Key Laboratory of Oasis Ecology, Xinjiang University, Urumqi 830046, China*
[3]*Nansen-Zhu International Research Center, Institute of Atmospheric Physics, Chinese Academy of Sciences, Beijing 100029, China*
[4]*Collaborative Innovation Center on Forecast and Evaluation of Meteorological Disasters, Nanjing University of Information Science and Technology, Nanjing 210044, China*

Correspondence should be addressed to Jianjun Yang; yjj@xju.edu.cn

Received 9 November 2020; Revised 21 February 2021; Accepted 19 March 2021; Published 5 April 2021

Academic Editor: Budong Qian

There are water resource shortages and frequent drought disasters in the arid region of northwestern China (ARNC). The purpose of this study is to understand the spatiotemporal variations of the droughts in this region and to further estimate future changes. Multiple drought indexes such as the standardized precipitation index (SPI), the standardized precipitation evapotranspiration index (SPEI), and the self-calibrated Palmer drought severity index (SC-PDSI) are used to investigate the temporal and spatial characteristics of the ARNC drought from 1950 to 2012. Our results indicate the following: (1) The drought indexes exhibit significant increasing trends, and the highest drought frequency occurred in the 1960s, followed by a decreasing trend during the next few decades. All four seasons exhibit a wet trend, with a higher drought frequency in summer than in the other seasons. (2) The changes of the drought indexes in the ARNC also exhibit distinct spatial variations, with a wet trend in the subregions of North Xinjiang (NXJ), the Tianshan Mountains (TS), South Xinjiang (SXJ), and the Qilian Mountains (QL), but with a dry trend in the subregions of the Hexi Corridor (HX) and the western part of Inner Mongolia (WIM). (3) There was a major climate variability in the ARNC that occurred in the 1980s, and there were dry and wet climate oscillation periods of 8a, 17a, and >20a.

1. Introduction

Drought is a major natural disaster on a global scale, and severe droughts can cause many other environmental problems. In the context of global warming, these problems are becoming more prominent [1, 2]. The frequency of moderate and extreme droughts in China has increased since the 1990s, and the area experiencing drought is expanding at a rate of 3.72% per decade [3]. Since 1978, the area affected by droughts in China has been increasing rapidly, and the total area of crop failure caused by droughts has also been increasing [4]. As the main arid climate region in China, the arid region in northwestern China (ARNC) is deeply landlocked, and its precipitation is constrained by the combinations of the monsoon and high-latitude atmospheric circulation [5, 6]. It is also one of the regions that is most sensitive to global warming [7, 8]. Water scarcity and persistent drought are the main factors limiting local sustainable development, and the droughts have also caused economic losses in this area. Therefore, an in-depth analysis of the spatiotemporal variations of the droughts in the ARNC is of great significance to local agricultural, ecological, and socioeconomic development.

Drought indexes have been widely used to describe the degree of drought. In recent years, the application of drought indexes has included monitoring droughts, assessing droughts, and predicting droughts, and drought indexes can also be used to assess the effects of droughts on meteorology, agriculture, and hydrology [9–13]. The standardized

precipitation index (SPI), the standardized precipitation evapotranspiration index (SPEI), and the Parmer drought severity index (PDSI) have been widely used to monitor drought events. The PDSI is calculated using monthly temperature and precipitation data and information on the water-holding capacity of the soils, which makes it a powerful tool for identifying droughts [14]. The self-calibrated Parmer drought severity index (SC-PDSI), which is based on the PDSI, is considered to be more suitable for global drought monitoring because it automatically calibrates itself at any location using dynamically computed values instead of empirical constants [15]. The SPI only uses precipitation data to estimate drought duration, scale, and intensity [16, 17]. It is easy to use and calculate for drought monitoring and assessment in different regions and on different time scales. Vicente-Serrano et al. [18] established the standard precipitation evapotranspiration index (SPEI), which is an index that characterizes the probability of the difference between the precipitation and evapotranspiration in a certain period of time. It has two advantages, namely, multi-scale features and sensitivity to changes in the evapotranspiration demand [19], and thus, it is widely used worldwide.

Most previous studies used a single drought index to investigate the drought variability in the ARNC [20–22]. However, the use of multiple drought indexes is also one of the main methods of monitoring drought conditions and of guiding early warning assessments [23]. Scholars such as Tang et al. and Yao et al. [24–26] used the SPI and SPEI to analyze the changes in and effects of droughts in different provinces of China. Most previous studies concentrated on the southwestern and eastern regions of China [27–29] where meteorological observation stations are densely distributed. Much less research has been conducted on northwestern China due to the sparse distribution of the meteorological stations in this region. Therefore, it is necessary to conduct a comprehensive analysis of the various drought indexes and compare the results to analyze the spatial and temporal changes in drought in the ARNC in order to improve our understanding of the variations in the drought in this region.

In this study, we analyzed the drought changes in the ARNC from 1950 to 2012 using the SPI, SPEI, and SC-PDSI in terms of the temporal trend, spatial trend, abrupt variation, and periodicity. In addition, a comparison of the analysis results of the three selected indexes was conducted to reveal the ability of each index to monitor the drought changes and characteristics in the ARNC to a certain extent. Through the mutual comparison of the different drought indexes, we can gain a deeper understanding of the drought variation characteristics in the study area. The results of this study provide a scientific basis for drought disaster prevention and mitigation in the ARNC.

2. Study Area and Methods

2.1. Study Area. The ARNC is located in the heart of the Eurasian continent (73–107°E and 35–50°N). The study area includes the entire Xinjiang Uygur Autonomous Region, the Hexi Corridor in Gansu Province, the Qilian Mountains, the Alxa Plateau in Inner Mongolia, and a small part of Western Ningxia Province, accounting for about one-quarter of the land area of China. The ARNC is surrounded by high mountains and has an average annual precipitation of less than 230 mm [30]. Moreover, the potential amount of evapotranspiration is extremely high, making this a classic water-scarce area. This region can be divided into six subregions based on the topographical features and climate features, following the method used in previous studies [31, 32]: North Xinjiang (NXJ), the Tianshan Mountains (TS), South Xinjiang (SXJ), the Qilian Mountains (QL), the Hexi Corridor (HX), and the Western part of Inner Mongolia (WIM) (Figure 1).

2.2. Drought Indexes. The SPI and SPEI can be calculated at different monthly scales, with typical values of 1, 3, 6, 12, and 24 months. In this study, we mainly analyzed the annual and interdecadal variations in drought, so a 12-month time scale was selected for the SPI and SPEI, combined with SC-PDSI, to analyze the drought variations using multiple drought indexes. The drought indexes and the corresponding datasets used in this paper are described below:

(1) SPI: The SPI from the Global Land Surface (1949–2012) dataset was obtained from the National Center for Atmospheric Research (NCAR), and it was calculated based on the Climate Research Unit (CRU) TS3.23/TS4.03 monthly precipitation data, with a spatial resolution is $1^{o} \times 1^{o}$ [33].

(2) SPEI: The SPEI dataset (1901–2015) was obtained from the Spanish National Research Council (CSIC), and it was calculated based on the CRU TS3.24.01 monthly data. The amount of potential evapotranspiration was calculated using the Penman-Monteith formula, and the spatial resolution is $0.5^{o} \times 0.5^{o}$ [34].

(3) SC-PDSI: The global SC-PDSI dataset for 1901–2018 was obtained from the CRU, and it was calculated based on the CRU TS4.03 monthly data. The potential evapotranspiration was calculated using the Penman-Monteith method, with a spatial resolution of $0.5^{o} \times 0.5$ [35, 36].

According to the national standards of the People's Republic of China, *Grades of meteorological drought GB/T20481-2017* [37], the criteria for drought classifications for each drought index are listed in Table 1.

2.3. Methods. Based on the availability of the dataset products, we chose the time series from 1950 to 2012 for use in this study. In order to obtain the three drought indexes at the same resolution, the bilinear interpolation method was used to interpolate the $1^{o} \times 1^{o}$ resolution SPI data to the $0.5^{o} \times 0.5^{o}$ resolution of the other two indexes. To study the changes in the drought indexes in depth, a variety of analysis methods were adopted.

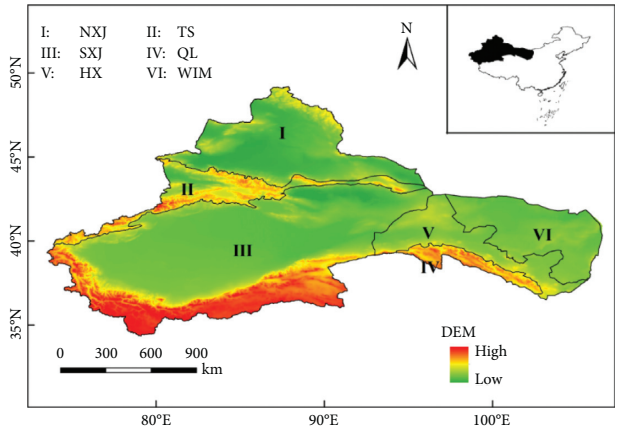

Figure 1: The locations of the study area and the six subregions.

Table 1: Drought classifications for SPI, SPEI, and SC-PDSI.

Drought level	SPI/SPEI	SC-PDSI
No drought	>−0.5	>−1
Drought	≤−0.5	≤−1

2.3.1. Sen's Slope Estimator. The Theil-Sen Median method, also known as Sen's slope estimation, is a robust non-parametric statistical trend calculation method [38]. This method can significantly reduce the influence of outliers and has a high computational efficiency. It is often used for trend analysis of long-term series data. The Sen's slope method is often used in combination with the Mann-Kendall trend test to determine the significance of a sequence trend [39–41].

2.3.2. Mann-Kendall Test. The Mann-Kendall trend test is another non-parametric method for detecting the significance of the trends of climate variables [42, 43]. In this study, we used Sen's slope to judge the increase or decrease in the drought index and used the M-K trend test to determine whether the trend passes the 0.5 significance level (hereinafter referred to as Sen + M-K trend analysis). When the Sen's trend degree is $\beta > 0$, the time series exhibits an upward trend; and when $\beta < 0$, the time series exhibits a downward trend. Moreover, when the statistical quantity $|Zc| > 1.96$ in the M-K trend test, the trend passes the 0.05 significant level; otherwise, the trend does not pass the 0.05 significance level. A sequential Mann-Kendall test that estimates progressive (UF) and backward (UB) series was used to detect abrupt variation years in the study series [44, 45].

2.3.3. Other Methods. In addition, we studied the variations in the drought indexes using the linear regression method and the non-parametric Pettitt test method [46] in order to determine the abrupt variation year in the drought index time series. Morlet wavelet analysis [47–49] was used to characterize the periodic variations in the ARNC. Wavelet transformation can reflect the periodic changes in the drought indexes on different time scales and their distribution in the time domain. The midpoint of the contours is the dry/wet transition, with positive wavelets representing wet conditions and negative wavelets representing dry conditions. The wavelet variance reflects the distribution of the fluctuation energy of the drought index time series with the time scale (a). It can be used to determine the main oscillation period in the wet and dry evolution process.

3. Results

3.1. Temporal Variations. Figure 2 shows the variations of SPI, SPEI, and SC-PDSI from 1950 to 2012 and the characteristics of the drought episodes in the ARNC. The changes in the drought index indicate that the evolutions of each series are similar. The trend analysis of the three drought indexes in the ARNC was performed using different methods. Table 2 shows that the drought indexes' values in the ARNC have increased over the past 63 years. Statistically significant upward trends were observed for the SPI (0.08/10 a), the SPEI (0.07/10 a), and the SC-PDSI (0.19/10 a) in the ARNC from 1950 to 2012. The results of the Sen + M-K trend analysis of the time series of the drought indexes indicate that the Sen slopes β of the SPI, SPEI, and SC-PDSI are >0, and $|Zc| > 1.96$. Therefore, the time series of the drought indexes have statistically significant increasing trends. Based on the results of these two methods, the overall trend in the ARNC from 1950 to 2012 was a dry to wet trend, which was consistent with the results of previous studies of the surface water resources and potential evapotranspiration in the ARNC [25, 50].

3.1.1. Interdecadal Variations. The interdecadal variation in the drought frequency for each drought index is shown in Figure 3. At the decadal scale, the 1960s was the driest period in the ARNC during 1950–2012, with the drought frequency of the SC-PDSI being as high as 74%, and the average drought frequencies of the three drought indexes were greater than 50%. The variations in the drought frequencies of the three drought indexes from 1950s to 1980s were consistent, but the drought frequencies of the SPEI and SC-PDSI changed from decreasing to increasing from the 1990s to the beginning of the 21st century, while the drought frequency of the SPI decreased from the 1980s to the beginning of the 21st century, showing inconsistency between the SPEI and SC-PDSI.

3.1.2. Seasonal Variations. In this section, the seasonal changes in the drought indexes were analyzed and the frequency of drought occurrence was calculated separately for each season. As can be seen from Figure 4, the trends of the drought indexes increased in each season, indicating that the climate became wetter in all of the seasons. The seasonal variations are consistent with the overall annual trend. In the summer, the increasing trends in the SPI, SPEI, and SC-PDSI were 0.21/10 a, 0.18/10 a, and 0.45/10 a, respectively (Figures 4(d)–4(f)), which were lower than in the other seasons and were not significant at the 0.05 level. The three drought indexes exhibited the most consistent trends in the spring, with increasing trends passing the 0.05 significance level. The wetting trends described by the SPI and SPEI were more consistent in each season, while the increasing trend of

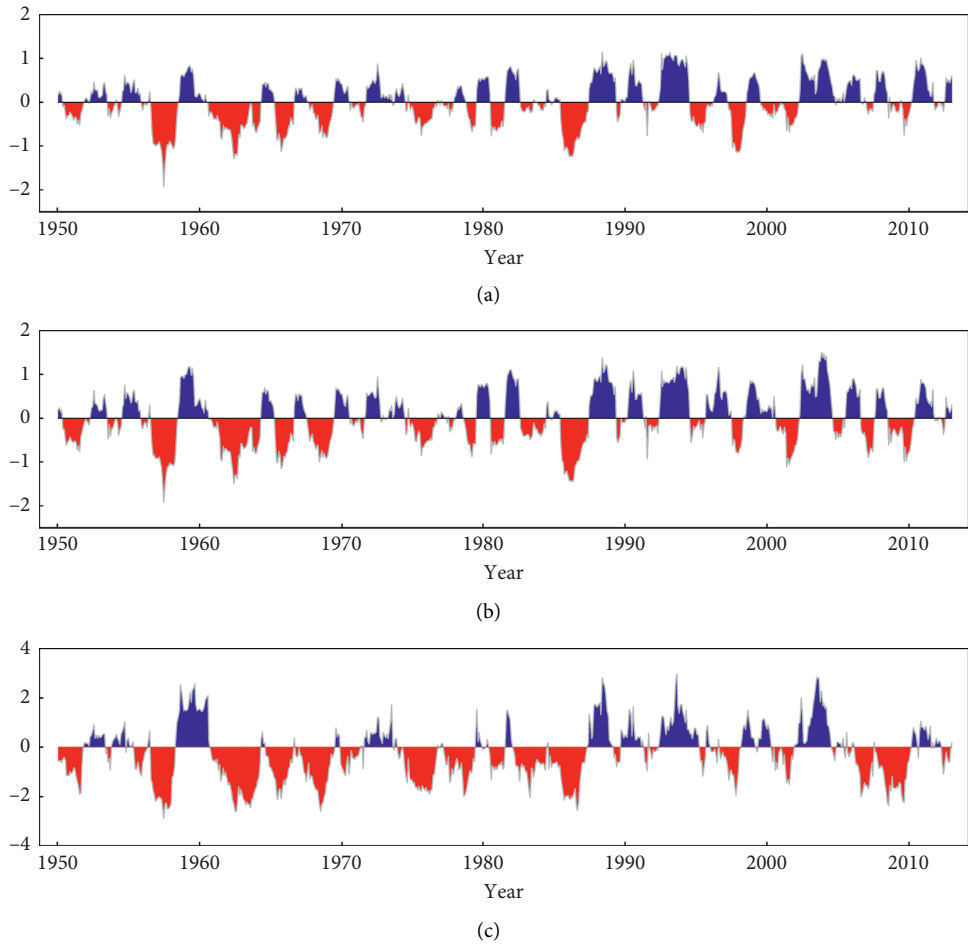

Figure 2: Evolution of the SPI, SPEI, and SC-PDSI in the ARNC during 1950–2012. (a) SPI. (b) SPEI. (c) SC-PDSI.

Table 2: Trend analysis and Sen + M-K trend analysis of the SPI, SPEI, and SC-PDSI.

Drought index	Propensity rate (/10 a)	Sen + M-K trend analysis		
		β	|Zc|	Trend
SPI	0.08*	0.001 > 0	>1.96	↑*
SPEI	0.07*	0.001 > 0	>1.96	↑*
SC-PDSI	0.19*	0.002 > 0	>1.96	↑*

*0.05 significance level.

the SC-PDSI in each season was somewhat greater than those of the SPI and SPEI.

The drought frequencies in each season indicate that the SPI had the highest frequency in fall and the lowest frequency in spring (Table 3). The SPEI had the highest drought frequency in winter, followed by fall, and the lowest frequency in spring. The SC-PDSI had the highest frequency in summer, followed by fall, winter, and spring. According to the averages of the three drought indexes in each season, the ARNC was mainly dominated by summer droughts, with a frequency of 28.7%, followed by fall (28.33%) and winter (27.78%), and the drought frequency in spring was the lowest (23.15%).

3.2. Spatial Variations. According to the results of the drought index trend analysis for each subregion (Figures 5(a)–5(c)), there were obvious regional differences in the drought changes in the ARNC. The pie charts show the percentage of the grids with different trends. As can be seen, the SPI, SPEI, and SC-PDSI have significant increasing trends with proportions of 69.9%, 64.1%, and 51.6%, respectively, especially in the NXJ, the TS, and most of the SXJ. The areas in which the drought indexes decreased were mainly concentrated in the HX, the WIM, and the southwestern part of the SXJ, and thus, the climate in these areas became drier. The analyses of the SPEI and SPI were similar, and the sum of the percentages of the slight decrease and the significant decrease was less than 15.0%. However, the SC-PDSI significantly decreased the grid percentage by as much as 29.1%, especially for the analysis of dry and wet changes in the QL, which was different from the SPI and SPEI. Therefore, the SC-PDSI was more serious in terms of the drought judgment in the ARNC.

The drought indexes in the NXJ, TS, SXJ, and QL subregions all had significant increasing trends (Table 4). Except for the slightly increasing results of the Sen + M-K trend test of the SC-PDSI in the HX subregion, the HX and WIM subregions mainly exhibited drought index decreasing

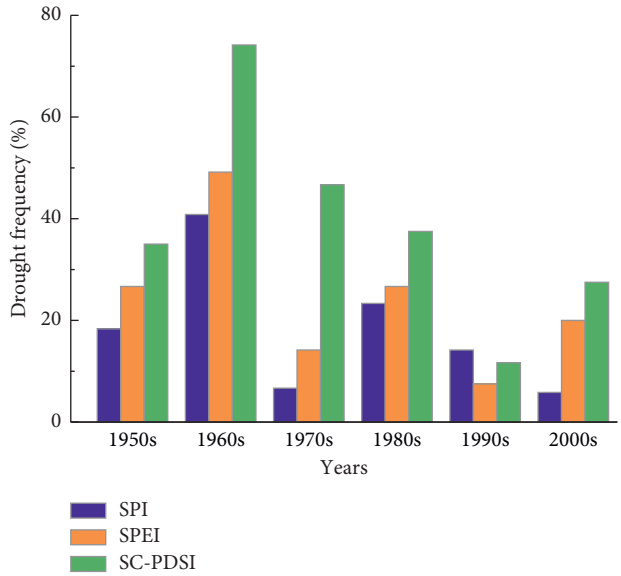

Figure 3: Interdecadal variations in the drought frequency in the ARNC.

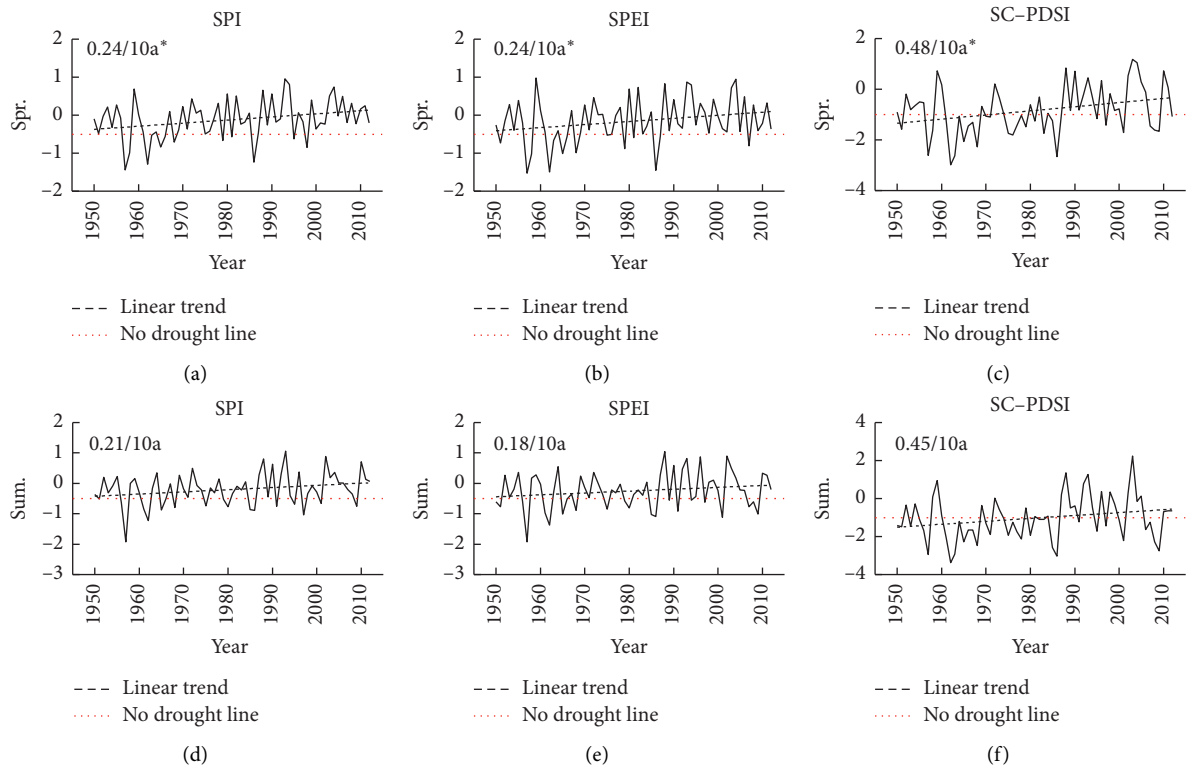

Figure 4: Continued.

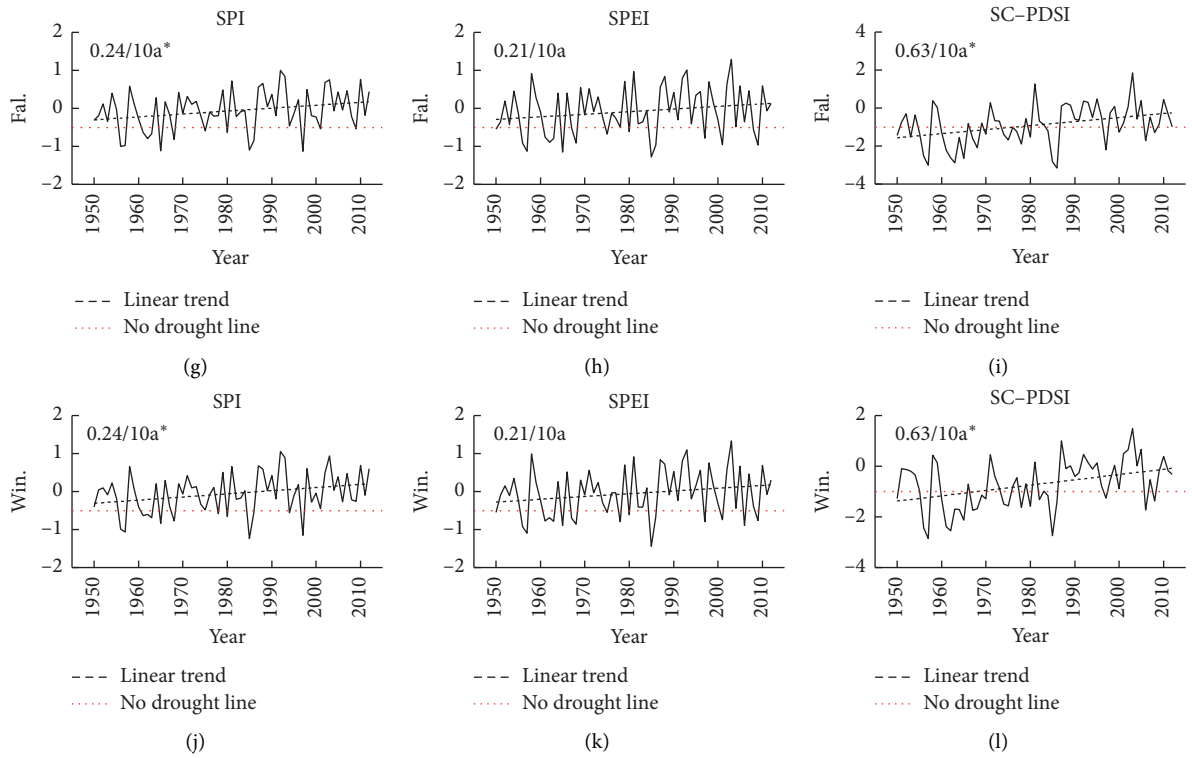

Figure 4: Seasonal changes in the drought indexes in (a–c) spring, (d–f) summer, (g–i) autumn, and (j–l) winter. *0.05 significance level.

Table 3: Frequency of droughts in each season (%).

Season	SPI	SPEI	SC-PDSI	Average drought frequency
Spr.	13.89	19.44	36.11	23.15
Sum.	18.89	22.78	44.44	28.70
Fall.	21.11	25.56	38.33	28.33
Win.	18.89	28.33	36.11	27.78

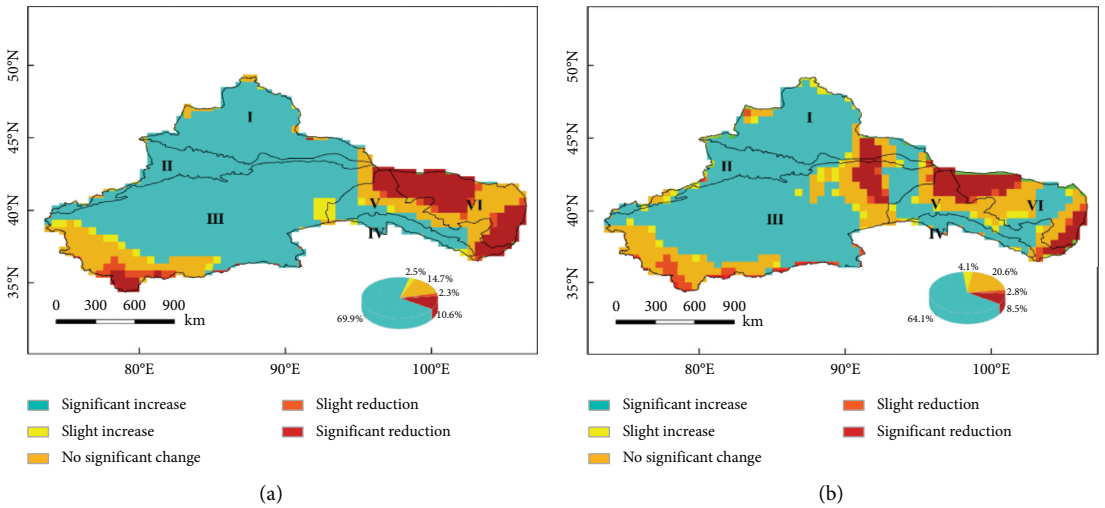

Figure 5: Continued.

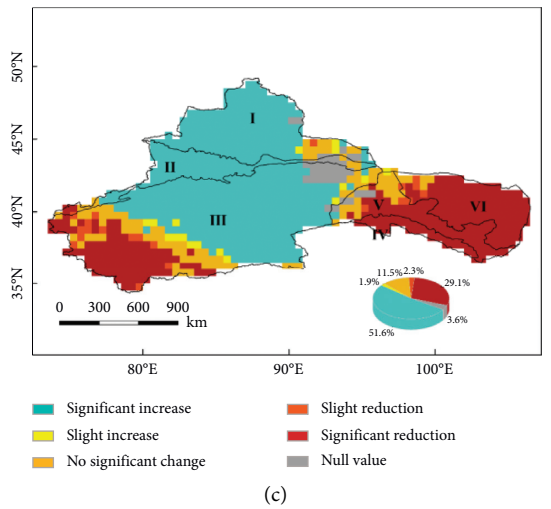

(c)

Figure 5: Spatial variations in the drought indexes in the ARNC. (a) SPI. (b) SPEI. (c) SC-PDSI.

Table 4: Sen + M-K test for the changes in the SPI, SPEI, and SC-PDSI in each subregion.

Subregion	Drought index	β	|Zc|	Trend
I	SPI	0.013 > 0	>1.96	↑*
	SPEI	0.012 > 0	>1.96	↑*
	SC-PDSI	0.031 > 0	>1.96	↑*
II	SPI	0.012 > 0	>1.96	↑*
	SPEI	0.012 > 0	>1.96	↑*
	SC-PDSI	0.026 > 0	>1.96	↑*
III	SPI	0.009 > 0	>1.96	↑*
	SPEI	0.009 > 0	>1.96	↑*
	SC-PDSI	0.022 > 0	>1.96	↑*
IV	SPI	0.011 > 0	>1.96	↑*
	SPEI	0.013 > 0	>1.96	↑*
	SC-PDSI	0.033 > 0	>1.96	↑*
V	SPI	−0.001 < 0	≤1.96	↓
	SPEI	−0.001 < 0	≤1.96	↓
	SC-PDSI	0.009 > 0	≤1.96	↑
VI	SPI	−0.007 < 0	≤1.96	↓
	SPEI	−0.003 < 0	≤1.96	↓
	SC-PDSI	−0.005 < 0	≤1.96	↓

*0.05 significance level.

trends. With global climate change, the East Asian monsoon continues to weaken, making the eastern part of northwestern China affected by the monsoon even drier [51]. The ARNC experienced a gradually increasing wetting trend from southeast to northwest. The increasing trend in precipitation in the ARNC changes from southeast to northwest [52], and the spatial changes in the ARNC's climate described by the three drought indexes are consistent with the spatial changes in precipitation.

3.3. Variation Characteristics

3.3.1. Abrupt Dry/Wet Variation Characteristics. Table 5 presents the results of the analysis of the M-K abrupt variation test and the Pettitt abrupt variation test for the three drought indexes from 1950 to 2012. In the ARNC, the M-K abrupt variation tests showed that the drought indexes exhibited variability in the 1980s, and the abrupt variations of the SPI, SPEI, and SC-PDSI occurred in 1987, 1980, and 1983, respectively. The results of Pettitt's abrupt variation test were more consistent, that the year of conversion from dry to wet for the SPI, SPEI, and SCPDSI was 1987. For each subregion, the abrupt variation points in the entire Xinjiang region as well as in the HX and WIM subregions were concentrated in the 1980s. The drought indexes in the NXJ, TS, and SXJ subregions exhibited increasing trends after 1980s, while the trends in the drought indexes in the HX and WIM subregions changed from increasing to decreasing trends. The abrupt variation in the QL subregion occurred in the 1970s, with an increasing trend in the drought indexes compared to the earlier period.

Table 5: Analysis of the catastrophe points of the SPI, SPEI, and SC-PDSI.

Study area	SPI				SPEI				SC-PDSI			
	M-K		Pettitt		M-K		Pettitt		M-K		Pettitt	
I	1987	−/+	1987	−/+	1984	−/+	1984	−/+	1987	−/+	1987	−/+
II	1993	−/+	1987	−/+	1987	−/+	1987	−/+	1987	−/+	1987	−/+
III	1981	−/+	1987	−/+	1980	−/+	1987	−/+	1977	−/+	1987	−/+
IV	1978	−/+	1972	−/+	1976	−/+	1972	−/+	1978	−/+	2002	−/+
V	1985	+/−	1985	+/−	1985	+/−	1985	+/−	1990	+/−	1967	+/−
VI	1982	+/−	1982	+/−	1981	+/−	1982	+/−	1972	+/−	1980	+/−
ARNC	1987	−/+	1987	−/+	1980	−/+	1987	−/+	1983	−/+	1987	−/+

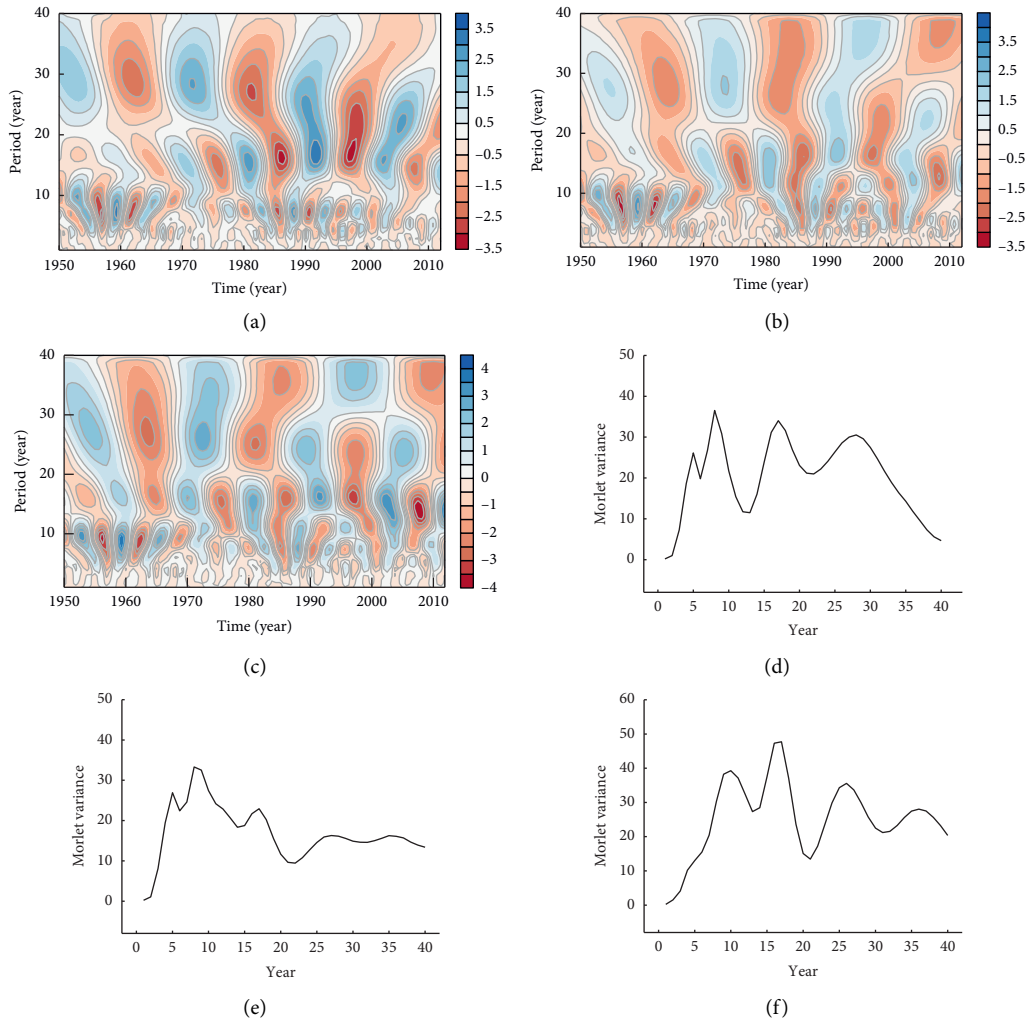

Figure 6: Continued.

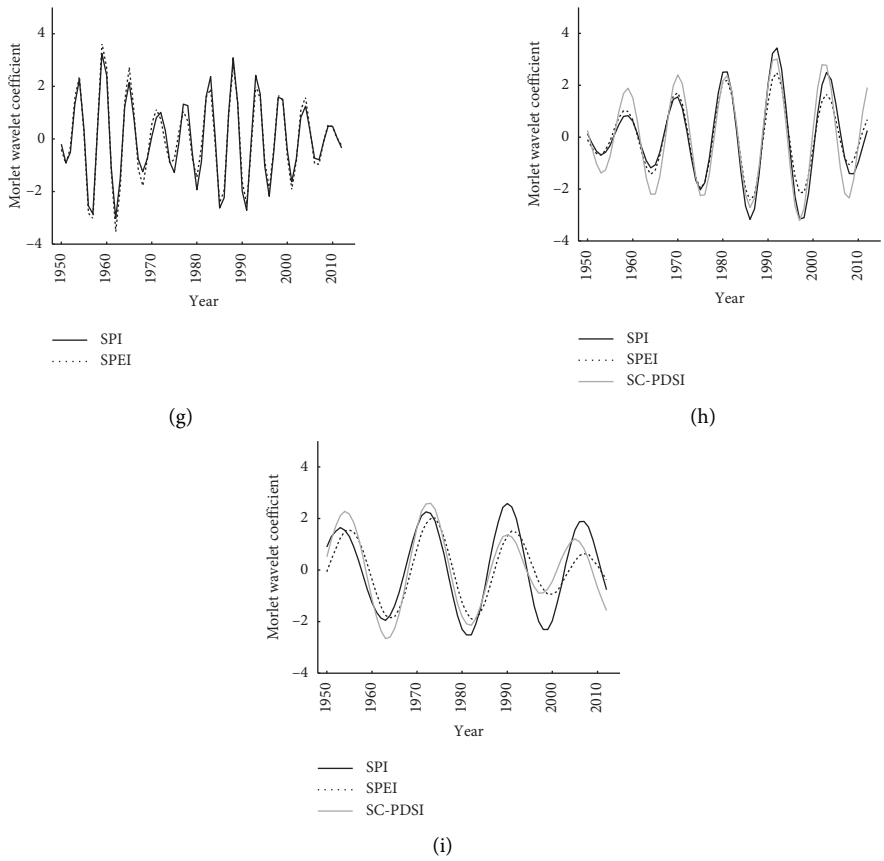

Figure 6: (a–c) Wavelet transformation and (d–f) wavelet variance of the SPI, SPEI, and SC-PDSI, and (g–i) wavelet coefficient during the 8a, 17a, and >20 a oscillation period in the ARNC from 1950 to 2012.

This confirms that there was a variation in the climate from dry to wet in the ARNC in the 1980s. Taking into account the atmospheric circulation factors, the South Asian monsoon has increased and the westerly winds have weakened since the 1980s, resulting in more moisture being transported from the Indian Ocean to the arid zone [53]. However, the changing trends for the subregions after the transition period were not the same.

3.3.2. Periodic Variation Characteristics. In order to identify the periodicity of the drought variations in the ARNC from 1950 to 2012, the wavelet transformation and wavelet variance based on the drought indexes are shown in Figure 6. In the ARNC, a phase of dry-wet transformation was observed at different time scales during the 63 years study period. There were obvious short (5–20a) and long (>20a) cycles in the wet and dry variations (Figures 6(a)–6(c)). Based on the wavelet variance analysis results (Figures 6(d)–6(f)), the SPI had oscillatory periods of 8a, 17a, and 28a, but there may be longer oscillatory periods that were not observed due to the length of the drought index time series data. The 8a oscillatory period was also observed for the SPEI, and the 8a oscillatory period occurred from 1951 to 2012. The SPI and SPEI experienced ten very consistent alternating dry-wet cycles during the 8a oscillation period (Figure 6(g)). The 17a oscillation period is the most obvious period for the SC-PDSI and is the main period for the SPI and SPEI. The SPI, SPEI, and SC-PDSI exhibited five dry-wet cycles during the 17a oscillation period, including five wet periods and five dry periods (Figure 6(h)). For the periodic variations of this time scale, the three indexes were very consistent. All three indexes exhibited oscillation periods of >20 a, i.e., 28 a (SPI), 27 a (SPEI), and 26 a (SC-PDSI) (Figure 6(i)), and the drought indexes experienced three consistent alternating dry-wet cycles during the >20 a oscillation period. Based on the analysis results for the three drought indexes, there were oscillation periods of 8a, 17a, and >20a in the dry-wet phase changes in the ARNC during the 63 years (1950 to 2012) study period, but larger scale periods may also occur.

4. Discussion

As drought is a complex climatic phenomenon that is affected by many meteorological factors, multiple drought index analysis using the widely accepted SPI, SPEI, and SC-PDSI is important for drought monitoring in the ARNC.

The frequency of drought occurrence in the SPI is consistent with the changes in precipitation in the ARNC [54, 55], with a trend of increasing precipitation after the 1980s. A more obvious trend of increasing humidity throughout the region occurred in the 1990s, and a trend of increasing precipitation has occurred since 2000; however, the rate of the increase in precipitation has decreased. Based

on the increasing trends in temperature and evapotranspiration, and the decreasing trend in relative humidity [31, 55, 56], the changes in all of these climatic factors may have had a negative impact on the drought mitigation in the ARNC. Therefore, the results of the interdecadal drought frequency analysis based on the SPI, which only considered the variability in precipitation, revealed that the application of the SPI in the ARNC is limited.

Guo et al. [57] found that the drought changes in Central Asia are closely related to the El Niño-Southern Oscillation (ENSO). The ENSO can influence every element of the East Asian monsoon system through telecorrelation, and drought is often correlated with the teleconnection index [58]. Wang et al. [59] proposed that the drought evolution in the ARNC may be influenced by the North Atlantic Oscillation, the Arctic Oscillation, and the Northern Hemisphere Polar Vortex by studying the relationship between droughts and the teleconnection indices. Many factors lead to variations in drought, including natural and unnatural factors. The analysis of the reasons for abrupt variations in dry and wet climate is difficult because the drought indexes are calculated based on different principles and they consider different meteorological factors and the natural and unnatural factors affect the different meteorological factors.

Chen et al. [60, 61] found that the ARNC, which is particularly sensitive to global climate change, actually experienced a major climate variability in the mid-1980s. However, the major factors responsible for this variation have not been identified. Due to the limitation of the length of the time series data, only the change period of the drought index over several decades has been analyzed. However, climate change is a long-term process, so it is necessary to continue to study the stable period of dry and wet variations over a longer time series in order to provide a scientific basis for future studies of climate variations.

5. Conclusions

The goal of this study was to use drought indexes to analyze the temporal and spatial variations of the drought in the ARNC from 1950 to 2012. The main conclusions of this study are as follows:

(1) The ARNC experienced a wetting trend from 1950 to 2012, with the highest drought frequency occurring in the 1960s, followed by an overall downward trend. However, in the early 21st century, there was an upward trend in the drought frequency. The seasonal drought trend was consistent with the annual mean variations, with the highest drought frequency occurring in summer, followed by falland winter.

(2) There were significant regional differences in the drought changes in the ARNC, with the entire Xinjiang region and the QL subregion exhibiting a wetting trend, and the HX and WIM subregions exhibiting a weak drying trend.

(3) The ARNC and its subregions were having abrupt variations from dry to wet in the 1980s. There were periodic changes in the drought indexes from 1950 to 2012, with different oscillation periods of 8 a, 17 a, and >20 a.

Data Availability

The SPI for Global Land Surface (1949–2012) dataset is from the National Center for Atmospheric Research (NCAR) repository (https://rda.ucar.edu/datasets/ds298.0/). The SPEI base v.2.5 dataset is from the Spanish National Research Council (CSIC) repository (http://hdl.handle.net/10261/153475). The SC-PDSI for global land dataset is from the Climate Research Unit (CRU) repository (https://crudata.uea.ac.uk/cru/data/drought/).

Conflicts of Interest

The authors declare no conflicts of interest.

Authors' Contributions

W. H., Y. L., J. Y., and E. Y. conceptualized the study; W. H., Y. L., and J. Y. contributed to data curation; W. H. wrote the original draft; W. H., Y. L., J. Y., and E. Y reviewed and edited the article. All authors have read and agreed on the published version of the manuscript.

Acknowledgments

This research was supported by the National Natural Science Foundation of China (grant nos. 42075168 and 51269030).

References

[1] B. I. Cook, J. E. Smerdon, R. Seager, and S. Coats, "Global warming and 21st century drying," *Climate Dynamics*, vol. 43, no. 9-10, pp. 2607–2627, 2014.

[2] A. Dai, "Drought under global warming: a review," *Wiley Interdisciplinary Reviews: Climate Change*, vol. 2, no. 1, pp. 45–65, 2011.

[3] M. Yu, Q. Li, M. J. Hayes, M. D. Svoboda, and R. R. Heim, "Are droughts becoming more frequent or severe in China based on the Standardized Precipitation Evapotranspiration Index: 1951-2010?" *International Journal of Climatology*, vol. 34, no. 3, pp. 545–558, 2014.

[4] L. Xu and M. Li, "The evolution of drought in China and its impact on agriculture in recent years," *Agricultural Science and Technology Hunan*, vol. 12, no. 11, pp. 1699–1702, 2011.

[5] X. Liu, Z. Shi, Q. Guo, and Z. Wang, "Uplift of the northern Tibetan Plateau and evolutions of East Asian monsoon and Asian inland arid environments," *Chinese Journal of Nature*, vol. 36, no. 3, pp. 170–175, 2014, in Chinese with English abstract.

[6] R. Ding, J. Li, S. Wang, and F. Ren, "Decadal change of the spring dust storm in northwest China and the associated atmospheric circulation," *Geophysical Research Letters*, vol. 32, no. 2, pp. 89–94, 2005.

[7] Y. Ding, G. Ren, Z. Zhao et al., "Detection, causes and projection of climate change over China: an overview of recent progress," *Advances in Atmospheric Sciences*, vol. 24, no. 6, pp. 954–971, 2007.

[8] Y. Shi, Y. Shen, E. Kang et al., "Recent and future climate change in Northwest China," *Climatic Change*, vol. 80, no. 3-4, pp. 379–393, 2007.

[9] M. Pedro-Monzonís, A. Solera, J. Ferrer, T. Estrela, and J. Paredes-Arquiola, "A review of water scarcity and drought indexes in water resources planning and management," *Journal of Hydrology*, vol. 527, pp. 482–493, 2015.

[10] J. Byakatonda, B. P. Parida, D. B. Moalafhi, and P. K. Kenabatho, "Analysis of long term drought severity characteristics and trends across semiarid Botswana using two drought indices," *Atmospheric Research*, vol. 213, pp. 492–508, 2018.

[11] A. Dai, "Characteristics and trends in various forms of the palmer drought severity index during 1900-2008," *Journal of Geophysical Research*, vol. 116, 2011.

[12] K. Xu, D. Yang, H. Yang, Z. Li, Y. Qin, and Y. Shen, "Spatio-temporal variation of drought in China during 1961-2012: a climatic perspective," *Journal of Hydrology*, vol. 526, no. 526, pp. 253–264, 2015.

[13] D. Halwatura, N. Mcintyre, A. M. Lechner, and S. Arnold, "Capability of meteorological drought indices for detecting soil moisture droughts," *Journal of Hydrology: Regional Studies*, vol. 12, pp. 396–412, 2017.

[14] A. Dai, K. E. Trenberth, and T. Qian, "A global dataset of palmer drought severity index for 1870-2002: relationship with soil moisture and effects of surface warming," *Journal of Hydrometeorology*, vol. 5, no. 6, pp. 1117–1130, 2004.

[15] N. Wells, S. Goddard, and M. J. Hayes, "A self-calibrating palmer drought severity index," *Journal of Climate*, vol. 17, no. 12, pp. 2335–2351, 2004.

[16] H. Wu, M. J. Hayes, D. A. Wilhite, and M. D. Svoboda, "The effect of the length of record on the standardized precipitation index calculation," *International Journal of Climatology*, vol. 25, no. 4, pp. 505–520, 2005.

[17] S. M. Vicente-Serrano and J. I. López-Moreno, "Hydrological response to different time scales of climatological drought: an evaluation of the Standardized Precipitation Index in a mountainous Mediterranean basin," *Hydrology and Earth System Sciences*, vol. 9, no. 5, pp. 523–533, 2005.

[18] S. M. Vicente-Serrano, S. Beguería, and J. I. López-Moreno, "A multiscalar drought index sensitive to global warming: the standardized precipitation evapotranspiration index," *Journal of Climate*, vol. 23, no. 7, pp. 1696–1718, 2010.

[19] H. Wang, Y. Chen, and Y. Pan, "Characteristics of drought in the arid region of northwestern China," *Climate Research*, vol. 62, no. 2, pp. 99–113, 2015.

[20] Q. Zhang, J. Li, V. P. Singh, and Y. Bai, "SPI-based evaluation of drought events in Xinjiang, China," *Natural Hazards*, vol. 64, no. 1, pp. 481–492, 2012.

[21] P. Yang, J. Xia, Y. Zhang, C. Zhan, and Y. Qiao, "Comprehensive assessment of drought risk in the arid region of Northwest China based on the global palmer drought severity index gridded data," *Science of The Total Environment*, vol. 627, pp. 951–962, 2018.

[22] S. Tong, J. Zhang, Q. Lai, and R. Wu, "Spatiotemporal variations of drought in inner Mongolia over the past 50 years based on SPEI," in *Proceedings of the 7th Annual Meeting of Risk Analysis Council of China Association for Disaster Prevention*, Changsha, China, November 2016.

[23] M. Svoboda and B. Fuchs, *Handbook of Drought Indicators and Indices*, World Meteorological Organization, Geneva, Switzerland, 2016.

[24] C. Tan, J. Yang, and M. Li, "Temporal-spatial variation of drought indicated by SPI and SPEI in Ningxia hui autonomous region, China," *Atmosphere*, vol. 6, no. 10, pp. 1399–1421, 2015.

[25] J. Yao, Y. Zhao, and X. Yu, "Spatial-temporal variation and impacts of drought in Xinjiang (Northwest China) during 1961–2015," *PeerJ*, vol. 6, p. e4926, 2018.

[26] J. Yao, Y. Zhao, Y. Chen, X. Yu, and R. Zhang, "Multi-scale assessments of droughts: a case study in Xinjiang, China," *Science of The Total Environment*, Elsevier, vol. 630, pp. 444–452, 2018.

[27] D. Zuo, S. Cai, Z. Xu et al., "Spatiotemporal patterns of drought at various time scales in Shandong Province of Eastern China," *Theoretical and Applied Climatology*, vol. 131, no. 1-2, pp. 271–284, 2018.

[28] J. Yang, D. Gong, W. Wang, M. Hu, and R. Mao, "Extreme drought event of 2009/2010 over southwestern China," *Meteorology and Atmospheric Physics*, vol. 115, no. 3-4, pp. 173–184, 2012.

[29] S. Sun, Q. Li, J. Li et al., "Revisiting the evolution of the 2009-2011 meteorological drought over Southwest China," *Journal of Hydrology*, vol. 568, pp. 385–402, 2019.

[30] Y. Chen, Q. Yang, Y. Luo et al., "Ponder on the issues of water resources in the arid region of northwest China," *Arid Land Geography*, vol. 35, no. 1, pp. 1–9, 2012, in Chinese with English abstract.

[31] H. Deng, Y. Chen, X. Shi et al., "Dynamics of temperature and precipitation extremes and their spatial variation in the arid region of northwest China," *Atmospheric Research*, vol. 138, no. 138, pp. 346–355, 2014.

[32] X. Deng, Y. Liu, Z. Liu, and J. Yao, "Temporal-spatial dynamic change characteristics of evapotranspiration in arid region of Northwest China," *Acta Ecologica Sinica*, vol. 37, no. 9, pp. 2994–3008, 2017, in Chinese with English abstract.

[33] N. C. f. A. Research and U. C. f. A. Research, *Standardized Precipitation Index (SPI) for Global Land Surface (1949-2012)*, NCAR, Boulder, CO, USA, 2013.

[34] S. M. Vicente-serrano, S. Beguería, J. I. López-Moreno, M. Angulo, and A. El Kenawy, "A new global 0.5° gridded dataset (1901-2006) of a multiscalar drought index: comparison with current drought index datasets based on the palmer drought severity index," *Journal of Hydrometeorology*, vol. 11, no. 4, pp. 1033–1043, 2010.

[35] G. V. D. Schrier, J. Barichivich, K. R. Briffa, and P. D. Jones, "A scPDSI-based global data set of dry and wet spells for 1901–2009," *Journal of Geophysical Research: Atmospheres*, vol. 118, no. 10, pp. 4025–4048, 2013.

[36] J. Barichivich, T. J. Osborn, I. Harris, G. V. D. Schrier, and P. D. Jones, "Bulletin of the American meteorological society," *Drought [in "State of the Climate in 2018"]*, vol. 100, pp. S1–S306, 2018.

[37] C. Zhang, H. Liu, Y. Song et al., *Grades of Meteorological Drought GB/T20481-2017*, Beijing: China Standard Press, Beijing, China, 2017, in Chinese.

[38] S. P. Kumar, "Estimates of the regression coefficient based on kendall's tau," *Journal of the American Statal Association*, vol. 63, pp. 1379–1389, 1968.

[39] M. Gocic and S. Trajkovic, "Analysis of changes in meteorological variables using Mann-Kendall and Sen's slope estimator statistical tests in Serbia," *Global and Planetary Change*, vol. 100, pp. 172–182, 2013.

[40] C. Wu, Z. Xian, and G. Huang, "Meteorological drought in the Beijiang River basin, South China: current observations and future projections," *Stochastic Environmental Research and Risk Assessment*, vol. 30, no. 7, pp. 1821–1834, 2016.

[41] R. M. D. Silva, C. A. G. Santos, M. Moreira, J. Corte-Real, and I. C. Medeiros, "Rainfall and river flow trends using Mann-Kendall and Sen's slope estimator statistical tests in the Cobres River basin," *Natural Hazards*, vol. 77, no. 2, pp. 1205–1221, 2015.

[42] A. U. Rahman and M. Dawood, "Spatio-statistical analysis of temperature fluctuation using Mann–Kendall and Sen's slope approach," *Climate Dynamics*, vol. 48, no. 3, pp. 783–797, 2017.

[43] A. Al-Mashagbah and M. Al-Farajat, "Assessment of spatial and temporal variability of rainfall data using kriging, Mann kendall test and the Sen?s slope estimates in Jordan from 1980 to 2007," *Research Journal of Environmental and Earth Sciences*, vol. 5, no. 10, pp. 611–618, 2013.

[44] P. Yang, J. Xia, Y. Zhang, and S. Hong, "Temporal and spatial variations of precipitation in Northwest China during 1960-2013," *Atmospheric Research*, vol. 183, pp. 283–295, 2017.

[45] N. Yao, Y. Li, T. Lei, and L. Peng, "Drought evolution, severity and trends in mainland China over 1961-2013," *Science of The Total Environment*, vol. 616-617, pp. 73–89, 2018.

[46] I. Mallakpour and G. Villarini, "A simulation study to examine the sensitivity of the Pettitt test to detect abrupt changes in mean," *Hydrological ences Journal/Journal des ences Hydrologiques*, vol. 61, no. 2, 2015.

[47] A. Grinsted, J. C. Moore, and S. Jevrejeva, "Application of the cross wavelet transform and wavelet coherence to geophysical time series," *Nonlinear Processes in Geophysics*, vol. 11, no. 5/6, pp. 561–566, 2004.

[48] Q. Zhang, J. Chen, and S. Becker, "Flood/drought change of last millennium in the Yangtze Delta and its possible connections with Tibetan climatic changes," *Global and Planetary Change*, vol. 57, no. 3-4, pp. 213–221, 2007.

[49] C. Lai, X. Chen, Z. Wang et al., "Spatio-temporal variation in rainfall erosivity during 1960-2012 in the pearl river basin, China," *Catena*, vol. 137, no. 137, pp. 382–391, 2016.

[50] Y. Shi, Y. Shen, and R. Hu, "Preliminary study on signal, impact and foreground of climatic shift from warm-dry to warm-humid in Northwest China," *Journal of Glaciology and Geocryology*, vol. 24, no. 3, pp. 219–226, 2002, in Chinese with English abstract.

[51] J. Yao, Q. Yang, W. Mao, and Z. Liu, "Progress of study on variation of atmospheric water cycle factors over arid region in Northwest China," *Arid Zone Research*, vol. 35, no. 2, pp. 269–276, 2018, in Chinese with English abstract.

[52] Z. Ren and D. Yang, "Trend and characteristics of climatic change in arid region of Northwest China in resent 50 years," *Journal of Earth Sciences and Environment*, vol. 29, no. 1, pp. 99–102, 2007, in Chinese.

[53] M. Staubwasser and H. Weiss, "Holocene climate and cultural evolution in late prehistoric-early historic west Asia," *Quaternary Research*, vol. 66, no. 3, pp. 372–387, 2006.

[54] H. Wang, Y. Chen, and Z. Chen, "Spatial distribution and temporal trends of mean precipitation and extremes in the arid region, northwest of China, during 1960-2010," *Hydrological Processes*, vol. 27, no. 12, pp. 1807–1818, 2013.

[55] Y. Chen, Z. Li, Y. Fan, H. Wang, and H. Deng, "Progress and prospects of climate change impacts on hydrology in the arid region of northwest China," *Environmental Research*, vol. 139, pp. 11–19, 2015.

[56] Z. Li, Y. Chen, Y. Shen, Y. Liu, and S. Zhang, "Analysis of changing pan evaporation in the arid region of Northwest China," *Water Resources Research*, vol. 49, no. 4, pp. 2205–2212, 2013.

[57] H. Guo, A. Bao, T. Liu et al., "Spatial and temporal characteristics of droughts in Central Asia during 1966-2015," *Science of the Total Environment*, vol. 624, pp. 1523–1538, 2018.

[58] A. Dai, "Drought under global warming: a review," *Wiley Interdisciplinary Reviews Climate Change*, vol. 2, no. 1, pp. 45–65, 2011.

[59] H. Wang, Y. Chen, Y. Pan, and W. Li, "Spatial and temporal variability of drought in the arid region of China and its relationships to teleconnection indices," *Journal of Hydrology*, vol. 523, no. 523, pp. 283–296, 2015.

[60] Y. Chen, K. Takeuchi, C. Xu, Y. Chen, and Z. Xu, "Regional climate change and its effects on river runoff in the Tarim Basin, China," *Hydrological Processes*, vol. 20, no. 10, pp. 2207–2216, 2010.

[61] Y. Chen, H. Deng, B. Li, Z. Li, and C. Xu, "Abrupt change of temperature and precipitation extremes in the arid region of Northwest China," *Quaternary International*, vol. 336, no. 26, pp. 35–43, 2014.